Efficient B-splines Collocation Simulations of the SARS-CoV-2/Cancer within-host Model with Diffusion and Immunity

Rohit Goel[1], Neha Ahlawat[2], R.C. Mittal[3]
Department of Mathematics, Jaypee Institute of Information Technology, Noida INDIA

Abstract: The disease COVID-19 is caused by the acute severe respiratory syndrome coronavirus 2 (SARS-CoV-2) and first diagnosed in Wuhan China, has whipped the entire world in its grip and threatened the mankind to the biggest ever extent. A within-host reaction-diffusion mathematical model describing the dynamics of SARS-CoV-2 in cancer patients has been considered in this research paper. Numerical simulation techniques based on the cubic B-splines collocation are proposed to the approximate the solutions of reaction-diffusion model taken into the consideration. The reduced collocation forms of the partial differential equations in the model are first being solved by the method of lines by reducing to the systems of first order ordinary differential equations which in turn are solved by the two methods viz. first by the well-known Runge-Kutta method of order 4 and secondly by the hybrid block method. The simulated results obtained by the two techniques are being analyzed and compared. It is found that Runge-Kutta method exhibits stability problem. However, hybrid block method produces good results but takes more computation time. The computed results are depicted for four different cases.

Keywords: Coronavirus, Cancer, SARS-CoV-2, Reaction-Diffusion Model, Cubic B-Splines, Method of Lines, Hybrid Block method.

DOI:10.53555/ecb/2022.11.03.17

1. Introduction

SARS-CoV-2 also known as severe acute respiratory syndrome is a member of a big family of viruses that cause a respiratory disease called coronavirus (COVID-19). SARS-Cov-2 is highly contagious and transmit rapidly [1] in humans and some animals. COVID-19 has been declared as global health emergency pandemic [2] by World Health Organization (WHO). The outbreak [3-5] of novel coronavirus (2019-nCoV) has triggered the reiteration of SARS-CoV from almost two decades ago. The virus has now become the biggest ever challenge to the whole mankind. The proclaimed global pandemic of COVID-19 has left no aspect of human life unaffected. The pandemic has adversely impacted [6-13] on emotional, economic, social and educational aspects globally. The dynamics of this infectious disease could not be controlled so far. Recently [14-16] some clinical observations and the genetic features of this infectious disease have been reported. The COVID-19 is more vulnerable in the patients with some pre [17] diseases like diabetes, hypertension, chronic cardiovascular or kidney disease, suppressed immune system and cancer. The cancer patients [18-20] are comparatively at a higher risk of severity of COVID-19 due to their weak immunity. Lymphopenia [21] is one of the associated severe infections in SARS-CoV-2/cancer patients. Mathematical modelling [22-28] of the dynamics of the transmission of COVID-19 has the potential to put forward better and effective strategies for the early detection, control and the treatment of this deadly infectious disease. Such mathematical models describing the dynamics of this infection have the ability to predict the future interaction of the disease and the precautionary measures to be taken to slow down its pace of destroying our lives and peace. Mathematical modeling and their suitable analysis [29] can explore many observed and non-observed aspects that can be taken care of accordingly to overcome this pandemic situation. Developing the mathematical models considering the least assumptions and to evolve the simulation techniques with greatest precision are the two major challenges to the researchers working in this field. Shahid [30] et al. proposed and analyzed a spatio-temporal advection-reaction-diffusion COVID-19

[1] *Corresponding Author*, Research Scholar, Jaypee Institute of Information Technology, Noida & Assistant Professor, Deshbandhu College (University of Delhi) rohitdd777@gmail.com
[2] Assistant Professor, Jaypee Institute of Information Technology, Noida neha.ahlawat@mail.jiit.ac.in
[3] Professor, Jaypee Institute of Information Technology, Noida mittalrc@gmail.com

epidemic model. COVID-19 are mainly categorized in epidemiological models and within-host models. The within-host models mainly concern with the dynamics of the interplaying between SARS-CoV-2 and the infected host cells [31-32]. Very less attention has been paid on the within-host models. There is large potential to explore with spatial variations and the mobility of cells and viruses in the within-host models. *Elaiw et al.* [33] proposed a within-host SARS-CoV-2/cancer model with immunity and diffusion.

The reaction-diffusion mathematical models [34-39] are the semi-linear parabolic partial differential equations that correspond to numerous dynamical, physical, chemical and biological phenomena associated with to our daily life. These equations describe the behaviors and variation of density distributed concentrations under the supremacy of the two processes of local interactions of species and the diffusion which causes the spread of species in space. The solutions of reaction-diffusion models account to a huge range of self-dissipating spatial pattern [40] formations. These models assist in the better understanding of complex biological structures. Many researchers [41-46] have successfully performed the structure-preserving descriptive analysis for many similar infectious diseases.

In the present paper, a within-host [33] reaction-diffusion SARS-CoV-2/cancer model is being solved numerically by the cubic B-splines collocation methods. The reduced systems are solved by the well known Runge-Kutta method of order 4 and by the hybrid block method [55]. The results are then compared and analyzed for different setting of influential parameters. The splines [47] comprise of an ingenious framework to deal with the discretization and the interpolation problems. B-splines or the basis splines [54] are the piecewise continuous spline functions that has minimal support with respect to the given degree, smoothness and the domain partition. The scheme of collocation [48-53] of cubic B-splines have been successfully implemented for many non-linear partial differential equation models like coupled Burger's equations, convection-diffusion equations, etc. The achieved results are found to be in pretty agreement with those already available in the literature and whence the proposed collocation methods are emerged as a burning alternative over the traditional numerical simulation techniques to deal with the reaction-diffusion models mainly concerning with the dynamics of alike infectious diseases.

2. The Reaction-Diffusion Within-Host SARS-CoV-2/Cancer Mathematical Model

The within-host SARS-CoV-2/Cancer reaction-diffusion mathematical model with CTL and antibody immunity proposed under some standard assumptions by Elaiw et al. [33] describing the interactions of the nutrients, healthy nutrient cells, cancer cells, free SARS-Cov-2 particles, CTLs and antibodies responses is taken into consideration. The model takes the following form:

$$\frac{\partial A(x,t)}{\partial t} = D_A \Delta A(x,t) + \xi - \gamma A(x,t) - \eta_1 A(x,t) N(x,t) - \eta_2 A(x,t) C(x,t)$$

$$\frac{\partial N(x,t)}{\partial t} = D_N \Delta N(x,t) + \sigma_1 \eta_1 A(x,t) N(x,t) - \eta_3 N(x,t) V(x,t) - (\gamma + \gamma_1) N(x,t)$$

$$\frac{\partial C(x,t)}{\partial t} = D_C \Delta C(x,t) + \sigma_2 \eta_2 A(x,t) C(x,t) - \eta_4 C(x,t) W(x,t) - (\gamma + \gamma_2) C(x,t)$$

$$\frac{\partial V(x,t)}{\partial t} = D_V \Delta V(x,t) + \sigma_3 \eta_3 N(x,t) V(x,t) - \eta_5 V(x,t) Z(x,t) - (\gamma + \gamma_3) V(x,t)$$

$$\frac{\partial W(x,t)}{\partial t} = D_W \Delta W(x,t) + \sigma_4 \eta_4 (1-\rho_1) C(x,t) W(x,t) - (\gamma + \gamma_4) W(x,t)$$

$$\frac{\partial Z(x,t)}{\partial t} = D_Z \Delta Z(x,t) + \sigma_5 \eta_5 (1-\rho_2) V(x,t) Z(x,t) - (\gamma + \gamma_5) Z(x,t)$$

(2.1)

where $A(x,t), N(x,t), C(x,t), V(x,t), W(x,t), Z(x,t)$ respectively denote the concentrations of nutrients, healthy epithelial cells, cancer cells, free SARS-CoV-2 particles, cancer specific CTLs and SARS-CoV-2 specific antibodies at time $t > 0$ and position $x \in \Omega$, Ω being the connected and bounded domain with smooth boundary $\partial\Omega$. The diffusion coefficients of the compartments are denoted by $D_A, D_N, D_C, D_V, D_W, D_Z$

respectively. Δ denotes the one-dimensional Laplacian operator. ξ and γA are respectively the rates of production and that of decay of the nutrient. The nutrient is consumed by the healthy epithelial cells and the cancer cells at the rates of $\eta_1 AN$ and $\eta_2 AC$ respectively. After consuming nutrient, the healthy epithelial cells and the cancer cells grow at the rates of $\sigma_1\eta_1 AN$ and $\sigma_2\eta_2 AC$, die at the rates of $\gamma_1 N$ and $\gamma_2 C$. The healthy epithelial cells get infected with SARS-Cov-2 at the rate of $\eta_3 NV$ while the cancer cells are attacked by CTLs at the rate of $\eta_4 CW$. The infected epithelial cells produce the free SARS-CoV-2 particles at the rate of $\sigma_3\eta_3 NV$ while the neutralization by the antibodies and the death decreases these particles at the rates of $\eta_5 VZ$ and $\gamma_3 V$. Cancer cells stimulate CTLs at the rate of $\sigma_4\eta_4(1-\rho_1)CW$ while CTLs die at the rate of $\gamma_4 W$. Antibodies are produced to clear the free particles at the rate of $\sigma_5\eta_5(1-\rho_2)VZ$ and die at the rate of $\gamma_5 Z$. The impact of lymphopenia on the potency of cancer specific CTLs, and SARS-CoV-2 specific antibody immune responses are respectively measured in parameters ρ_1 and ρ_1. The parameters used in the model are assumed to be positive and are described in *Table 1* [33].

The biologically compatible initial conditions for the system (2.1) are given by:

$$A(x,0)=A_0(x), \qquad N(x,0)=N_0(x), \qquad C(x,0)=C_0(x)$$
$$V(x,0)=V_0(x), \qquad W(x,0)=W_0(x), \qquad Z(x,0)=Z_0(x) \tag{2.2}$$

The functions $A_0(x), N_0(x), C_0(x), V_0(x), W_0(x), Z_0(x)$ are non-negative and continuous in Ω.

The given model (2.1) is also associated with the following homogeneous Neumann boundary conditions.

$$\frac{\partial A}{\partial \vec{v}}=\frac{\partial N}{\partial \vec{v}}=\frac{\partial C}{\partial \vec{v}}=\frac{\partial V}{\partial \vec{v}}=\frac{\partial W}{\partial \vec{v}}=\frac{\partial Z}{\partial \vec{v}}=0, \qquad t>0, \qquad x\in\partial\Omega \tag{2.3}$$

3. Cubic B-spline interpolation

Let the one-dimensional domain of interest $[a,b]$ be partitioned uniformly by the knots x_i as: $a=x_0<x_1 \ldots < x_n=b$ and h is the uniform step size of the mesh given by:

$$h=x_i-x_{i-1}=\frac{b-a}{n}\,; i=1,2\ldots\ldots n$$

The solutions are approximated as $A^n(x,t), N^n(x,t), C^n(x,t), V^n(x,t), W^n(x,t), Z^n(x,t)$, respectively in the form given below:

$$A^{(n)}(x,t)=\sum_{i=-1}^{n+1} a_i(t)\,B_i(x), \qquad a<x<b,\ \ t>0 \tag{3.1}$$
$$N^{(n)}(x,t)=\sum_{i=-1}^{n+1} n_i(t)\,B_i(x), \qquad a<x<b,\ \ t>0 \tag{3.2}$$
$$C^{(n)}(x,t)=\sum_{i=-1}^{n+1} c_i(t)\,B_i(x), \qquad a<x<b,\ \ t>0 \tag{3.3}$$
$$V^{(n)}(x,t)=\sum_{i=-1}^{n+1} v_i(t)\,B_i(x), \qquad a<x<b,\ \ t>0 \tag{3.4}$$
$$W^{(n)}(x,t)=\sum_{i=-1}^{n+1} w_i(t)\,B_i(x), \qquad a<x<b,\ \ t>0 \tag{3.5}$$
$$Z^{(n)}(x,t)=\textstyle\sum_{i=-1}^{n+1} z_i(t)\,B_i(x), \qquad a<x<b,\ \ t>0 \tag{3.6}$$

where a_i, n_i, c_i, v_i, w_i and z_i are the time dependent coefficients of the approximated solutions to be determined from the boundary conditions and the collocation scheme.

Table 1: *Description of Parameters*

Parameters	***Description***	***Value***
ξ	Recruitment rate of nutrient	0.02
η_1	Uptake rate of nutrient by healthy epithelial cells	Varied
η_2	Uptake rate of nutrient by cancer cells	Varied
η_3	Infection rate of epithelial cells by virus	0.55
η_4	Killing rate of cancer cells by CTLs	Varied
η_5	Removal rate of viruses by antibodies	Varied
σ_1	Growth rate of epithelial cells	0.8
σ_2	Growth cells of cancer cells	0.8
σ_3	Production rate of virus	0.24
σ_4	Stimulation rate of CTLs	0.1
σ_5	Stimulation rate of antibodies	0.2
γ	Decay rate of nutrient	0.02
γ_1	Decay rate of epithelial cells	Varied
γ_2	Decay rate of cancer cells	Varied
γ_3	Decay rate of virus	Varied
γ_4	Decay rate of CTLs	Varied
γ_5	Decay rate of antibodies	Varied
ρ_1	Effect of lymphopenia on CTL immune responses	[0,1]
ρ_2	Effect of lymphopenia on antibody immune responses	[0,1]
D_A	Diffusion coefficient of nutrient	0.1
D_N	Diffusion coefficient of healthy epithelial cells	0.1
D_C	Diffusion coefficient of cancer cells	0.1
D_V	Diffusion coefficient of free SARS-CoV-2 particles	0.1
D_W	Diffusion coefficient of CTLs	0.1
D_Z	Diffusion coefficient of antibodies	0.1

The cubic B-spline basis functions $B_i(x)$ at the knots are defined by the following piecewise continuous polynomials:

$$B_i(x) = \frac{1}{h^3}\begin{cases} (x - x_{i-2})^3 & x \in [x_{i-2}, x_{i-1}) \\ (x - x_{i-2})^3 - 4(x - x_{i-1})^3 & x \in [x_{i-1}, x_i) \\ (x_{i+2} - x)^3 - 4(x_{i+1} - x)^3 & x \in [x_i, x_{i+1}) \\ (x_{i+2} - x)^3 & x \in [x_{i+1}, x_{i+2}) \\ 0 & otherwise \end{cases}$$

where the set of the functions $B_{-1}, B_0, B_1, \ldots\ldots\ldots B_N, B_{n+1}$ form a basis of cubic splines over the given domain $a \leq x \leq b$. The values of these basis functions $B_j(x)$ and their first two successive derivatives $B_i'(x), B_i''(x)$ over the defined set of knots are summarized in *Table 2.*

Table 2: *Values of B-spline Basis functions and their derivatives*

	x_{i-2}	x_{i-1}	x_i	x_{i+1}	x_{i+2}
$B_j(x)$	*0*	*1*	*4*	*1*	*0*
$B_i'(x)$	*0*	*-3/h*	*0*	*3/h*	*0*
$B_i''(x)$	*0*	$6/h^2$	$-12/h^2$	$6/h^2$	*0*

The approximate values of $A^{(n)}(x,t)$ and its derivatives at any time t and at a particular knot x_i can be expressed in terms of the quantities $a_i(t)$ as given below.

$$\left.\begin{aligned} A_i &= a_{i-1} + 4a_i + a_{i+1} \\ hA_i' &= 3(a_{i+1} - a_{i-1}) \\ h^2A_i'' &= 6(a_{i-1} - 2a_i + a_{i+1}) \end{aligned}\right\} \quad (3.7)$$

Similar treatment is to be performed for other variables. Here we denote A_i is the value of $A^{(n)}(x,t)$ at the *i-th* node x_i and so on.

4. Dealing Boundary Conditions

Given that the model is associated with the homogeneous Neumann boundary conditions:

$$\left(\frac{\partial A}{\partial x}\right)_{x=a} = 0 \quad \text{and} \quad \left(\frac{\partial A}{\partial x}\right)_{x=b} = 0$$

Then the proposed numerical scheme of collocation of cubic B-splines assumes boundary approximations of *A* that can be expressed as:

$$\begin{aligned} a_1 - a_{-1} &= 0 \\ a_{n+1} - a_{n-1} &= 0 \end{aligned} \tag{4.1}$$

so that, the values of the extrapolated coefficients a_{-1} and a_{n+1} are found.

$$\begin{aligned} a_{-1} &= a_1 \\ a_{n+1} &= a_{n-1} \end{aligned}$$

Thus, the two extrapolated time dependent coefficients a_{-1} and a_{n+1} falling outside the prescribed knots are determined. The other variables can also be dealt in the similar fashion at the boundary.

5. Estimation of Initial Vector

The initial vector can be estimated by using the given initial conditions and the boundary values of their derivatives.

$$A_x(a,0) = A_x(x_0,0) = 0$$

$$A(x_j,0) = A_0(x_j), \qquad j = 1,2 \dots \dots, n-1$$

$$A_x(b,0) = A_x(x_n,0) = 0$$

Similar expressions will be obtained for the other variables. Equation (3.1) yields a $(n+1)\times(n+1)$ following system.

$$A\,\widehat{a^0} = \widehat{\phi_1^0}$$

where

$$A = \begin{bmatrix} 4 & 2 & & & & & \\ 1 & 4 & 1 & & & & \\ & & \dots & \dots & \dots & & \\ & & \dots & \dots & \dots & & \\ & & & & 1 & 4 & 1 \\ & & & & & 2 & 4 \end{bmatrix}_{(n+1)\times(n+1)} \qquad \widehat{a^0} = \begin{bmatrix} a_0^0 \\ a_1^0 \\ \dots \\ \dots \\ \dots \\ a_{n-1}^0 \\ a_n^0 \end{bmatrix} \qquad \widehat{\phi_1^0} = \begin{bmatrix} A_0(x_0) \\ A_0(x_1) \\ \dots \\ \dots \\ \dots \\ A_0(x_{n-1}) \\ A_0(x_n) \end{bmatrix}$$

and so on. This reduced tri-diagonal system can thus be solved by Thomas algorithm [56-57] to achieve the initial time dependent coefficients.

6. Methods of Implementation

The proposed system (2.1) is being solved by collocation of cubic B-splines followed by the method of lines and the finite difference scheme respectively. The one-dimensional spatial domain of interest $[a,b]$ be partitioned uniformly by the knots x_i as: $a = x_0 < x_1 \dots < x_n = b$ and h is the uniform step size of the mesh given by:

$$h = x_i - x_{i-1} = \frac{b-a}{n}\,; i = 1,2 \dots \dots n$$

The one-dimensional spatial domain is portioned uniformly as performed in Section 3. Let the time period $[0,T]$ be uniformly discretized as $0 = t_0 < t_1 \dots < t_m = T$ with $k = \frac{T}{m}$ norm. Let $A_i^n, N_i^n, C_i^n, V_i^n, W_i^n, Z_i^n$ denote the

approximated values of $A(x,t), N(x,t), C(x,t), V(x,t), W(x,t), Z(x,t)$ respectively at the spatial node x_i and time $t_n = nk$.

This technique is basically used to solve partial differential equations using discretization in a dimension that results in the system of ordinary differential equations. The reaction-diffusion equation in system (2.1) for $A(x,t)$ can be expressed in the standard form as:

$$\frac{\partial A(x,t)}{\partial t} = D_A \frac{\partial^2 A}{\partial x^2} + \phi_1(A, N, C, V, W, Z)$$

where D_A is the diffusion coefficient and the corresponding term is the diffusion term and ϕ_1 represents the reaction term for the variable $A(x,t)$.

Using (3.1) and (3.7) for the approximate solution $A^n(x,t)$, the above equation reduces to the following system of ordinary differential equations in the time dependent quantities a_i:

$$\dot{a}_{i-1} + 4\dot{a}_i + \dot{a}_{i+1} = \frac{6D_A}{h^2}(a_{i-1} - 2a_i + a_{i+1}) + \phi_{1i}\,; \quad 0 \le i \le n$$

The dots represent the respective derivatives with respect to time t. Upon eliminating the extrapolated coefficients $\dot{a}_{-1}, \dot{a}_{n+1}, a_{-1}, a_{n+1}$, the following system of ordinary differential equations is obtained.

$$P\hat{\dot{\boldsymbol{a}}} = M_A \hat{\boldsymbol{a}} + \widehat{\phi_1}$$

where $M_A = \frac{6D_A}{h^2} B$

$$P = \begin{bmatrix} 4 & 2 & & & & & \\ 1 & 4 & 1 & & & & \\ & & \cdots & \cdots & \cdots & & \\ & & \cdots & \cdots & \cdots & & \\ & & & & 1 & 4 & 1 \\ & & & & & 2 & 4 \end{bmatrix}_{(n+1)\times(n+1)} \qquad B = \begin{bmatrix} -2 & 2 & & & & & \\ 1 & -2 & 1 & & & & \\ & & \cdots & \cdots & \cdots & & \\ & & \cdots & \cdots & \cdots & & \\ & & & & 1 & -2 & 1 \\ & & & & & 2 & -2 \end{bmatrix}_{(n+1)\times(n+1)}$$

and

$$\hat{\dot{\boldsymbol{a}}} = \begin{bmatrix} \dot{a}_0 \\ \dot{a}_1 \\ \cdots \\ \cdots \\ \cdots \\ \dot{a}_{n-1} \\ \dot{a}_n \end{bmatrix}, \qquad \widehat{\phi_1} = \begin{bmatrix} \phi_{10} \\ \phi_{11} \\ \cdots \\ \cdots \\ \cdots \\ \phi_{1(n-1)} \\ \phi_{1n} \end{bmatrix}_{(n+1)\times 1}$$

Here, P and M_A are tri-diagonal matrices of order $(n+1)$ and $\widehat{\phi_1}$ is the column vector *of* order $(n+1)$.

Now, Considering the complete simultaneous system (2.1) for approximating solutions, the following system is obtained:

$$U\frac{dX}{dt} = LX + F$$

where W and V are the corresponding block diagonal matrices each of order $6(n+1)$.

$$U = \begin{bmatrix} P & 0 & 0 & 0 & 0 & 0 \\ 0 & P & 0 & 0 & 0 & 0 \\ 0 & 0 & P & 0 & 0 & 0 \\ 0 & 0 & 0 & P & 0 & 0 \\ 0 & 0 & 0 & 0 & P & 0 \\ 0 & 0 & 0 & 0 & 0 & P \end{bmatrix}_{6(n+1)\times 6(n+1)}$$

$$L = \begin{bmatrix} M_A & 0 & 0 & 0 & 0 & 0 \\ 0 & M_N & 0 & 0 & 0 & 0 \\ 0 & 0 & M_C & 0 & 0 & 0 \\ 0 & 0 & 0 & M_V & 0 & 0 \\ 0 & 0 & 0 & 0 & M_W & 0 \\ 0 & 0 & 0 & 0 & 0 & M_Z \end{bmatrix}_{6(n+1)\times 6(n+1)}$$

Here *X* and *F* are the column vectors of time dependent numbers and the right-hand side quantities respectively.

$$X = \begin{bmatrix} \hat{a} \\ \hat{n} \\ \hat{c} \\ \hat{v} \\ \hat{w} \\ \hat{z} \end{bmatrix}, \qquad F = \begin{bmatrix} \widehat{\phi_1} \\ \widehat{\phi_2} \\ \widehat{\phi_3} \\ \widehat{\phi_4} \\ \widehat{\phi_5} \\ \widehat{\phi_6} \end{bmatrix}_{6(n+1)\times 1}$$

The parameter vector *X* in the above system of ordinary differential equations is determined at a specified initial time level using Thomas algorithm. The system is then separately solved by Runge-Kutta method of order 4 and Hybrid Block method respectively.

7. Hybrid Block Method

The foundations of the one-step hybrid block method derived by *Ramos et al.* [55] has been described in this section. Consider the equation of the form:

$$y' = f(t, y),\ y(t_0) = y_0 \qquad where\ t \in [t_0, t_n] \tag{6.1}$$

Consider the uniform partition $t_0 < t_1 < \cdots < t_n$ with fixed step size of *k*. Let the polynomial $p(t)$ gives an approximate solution of (1) with $m_j \in \mathbb{R}$ are the unknowns to be determined.

$$y(t) \approx p(t) = \sum_{j=0}^{4} m_j\, t^j \tag{6.2}$$

$$y'(t) \approx p'(t) = \sum_{j=1}^{4} j\, m_j\, t^{j-1} \tag{6.3}$$

Two intra-step points $t_{i+r} = t_i + rk$ and $t_{i+s} = t_i + sk$, $0 < r < s < 1$ are introduced to interpolate (6.2) at t_i and collocate (6.3) at $t_i, t_{i+r}, t_{i+s}\ and\ t_{i+1}$ that result into the following matrix form of the system of equations:

$$\begin{bmatrix} 1 & t_i & t_i^2 & t_i^3 & t_i^4 \\ 0 & 1 & 2t_i & 3t_i^2 & 4t_i^3 \\ 0 & 1 & 2t_{i+r} & 3t_{i+r}^2 & 4t_{i+r}^3 \\ 0 & 1 & 2t_{i+s} & 3t_{i+s}^2 & 4t_{i+s}^3 \\ 0 & 1 & 2t_{i+1} & 3t_{i+1}^2 & 4t_{i+1}^3 \end{bmatrix} \begin{bmatrix} m_0 \\ m_1 \\ m_2 \\ m_3 \\ m_4 \end{bmatrix} = \begin{bmatrix} y_i \\ f_i \\ f_{i+r} \\ f_{i+s} \\ f_{i+1} \end{bmatrix}$$

where $f_j = f(t_j, y_j)$ for $j = i, i+r, i+s, i+1$.

The system is thus solved to get the values of the unknown coefficients $m_j's$. In order to ensure the fourth order convergence, it can be shown that

$$y_{i+1} = y_i + \frac{k}{12}(f_i + 5f_{i+r} + 5f_{i+s} + f_{i+1})$$

with $r = \left(\frac{1}{2} - \frac{\sqrt{5}}{2}\right)$ and $s = \left(\frac{1}{2} + \frac{\sqrt{5}}{2}\right)$.

This one-step proposed hybrid block method is used to solve the system of first order ordinary differential equations obtained by the current collocation scheme of the given partial differential equations in (2.1).

8. Numerical Simulations

Depending upon the concerns of the biological aspects, the global existential stability of the proposed model and the equilibrium existence observations as available in the literature, numerical simulations are being performed for the four different cases. The following set [33] of the initial values have been considered:

$$A(x,0) = 0.5(1 + 0.3\,cos^2(\pi x))$$
$$N(x,0) = 0.1(1 + 0.3\,cos^2(\pi x))$$
$$C(x,0) = 0.05(1 + 0.3\,cos^2(\pi x))$$
$$V(x,0) = 0.02(1 + 0.3\,cos^2(\pi x))$$
$$W(x,0) = 0.004(1 + 0.3\,cos^2(\pi x))$$
$$Z(x,0) = 0.002(1 + 0.3\,cos^2(\pi x)) \qquad x \in [0,2]$$

The values of ρ_1 and ρ_2 are fixed to be zero. Depending upon the equilibrium points [33] with reference to their global stabilities, four different cases [33] have been discussed. The parameter values taken in these cases are given in *Table 3.*

Table 3: *Parameter Values*

	η_1	η_2	η_4	η_5	γ_1	γ_2	γ_3	γ_4	γ_5
$Case\ I$	0.1	0.1	0.9	0.3	0.01	0.0005	0.5	0.0005	0.07
$Case\ II$	0.3	0.2	0.03	0.3	0.02	0.02	0.0005	0.9	0.07
$Case\ III$	0.2	0.3	1.2	0.3	0.01	0.008	0.0005	0.0001	0.07
$Case\ IV$	0.9	0.5	1.7	1.7	0.0001	0.0003	0.0003	0.0001	0.0001

The simulations are being performed for the collocation schemes of cubic B-splines followed by the method of lines which when reduced to a system of ordinary differential equations are solved by the Runge-Kutta method of order 4 and the hybrid block method respectively. To discuss the stability and the accuracy of the proposed methods, results are visualised for different values of the time step size k. The consistency of the solutions for the proposed model is also established by varying parameters. All the simulations have been performed on Intel(R) Core (TM) i3-1005G1 CPU @ 1.20GHz 1.19 GHz 10-th Generation Processor with Visual Studio Code.

9. Results and Discussions

The numerical simulations have been performed and visualized for the different arrangements of the time step size $k = 0.01$ and 0.001 with $n = 21,\ 51$ and 101. The consistency and the accuracy of the solutions, obtained by solving the resulted systems by Runge-Kutta method and hybrid block method, have been discussed.

It is observed that for smaller value of *n*, the value of time step should be large. For $n = 21, k = 0.01$ results are quite good and satisfactory. The experiments are being performed and the results are being evaluated for $n = 51$ and 101 with time step $k = 0.001$.

It is found that for $n = 101, k = 0.001$, RK method fails to converge. However, for $n = 51, k = 0.001$, it gives results for some cases. Therefore, RK method is not suitable for numerical simulations implying the instability of the method for the given model. Therefore, simulations for $n = 51$ and $n = 101$ with $k = 0.001$ are being performed with the hybrid block method which gives quite good results for both. Further, the simulated results are in well reach with those available in [33]. The hybrid block method significantly provided accurate solutions with less computational efforts. The consistency of the simulated results is also established by varying parameters of the model.

Figure 1: Numerical Simulations for Case-I by Hybrid Block method at k=0.001, n=101

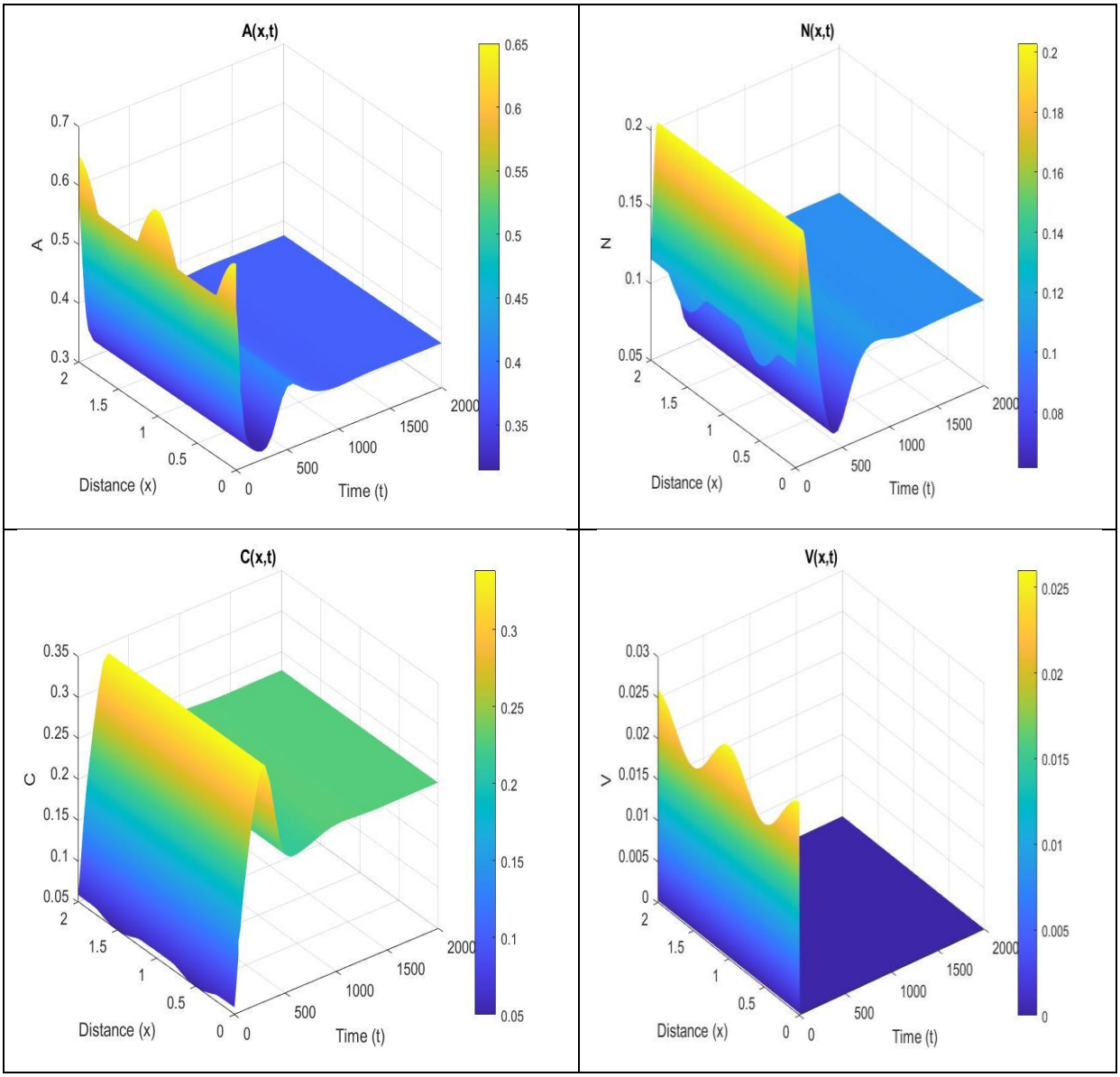

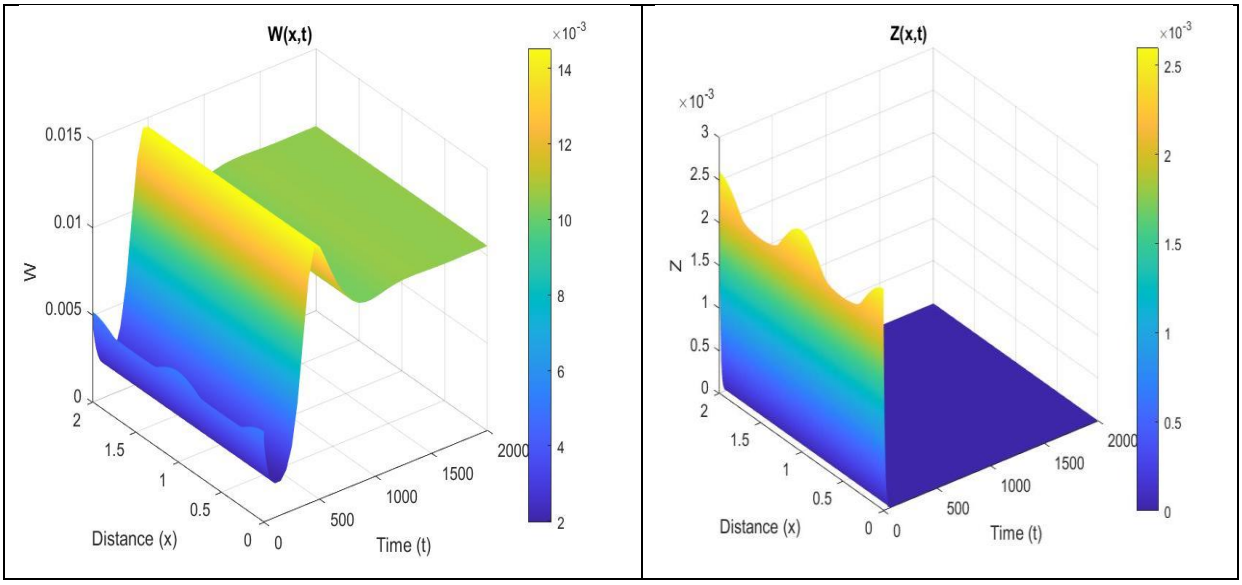

Figure 2: Numerical Simulations for Case-II by Hybrid Block method at k=0.001, n=101

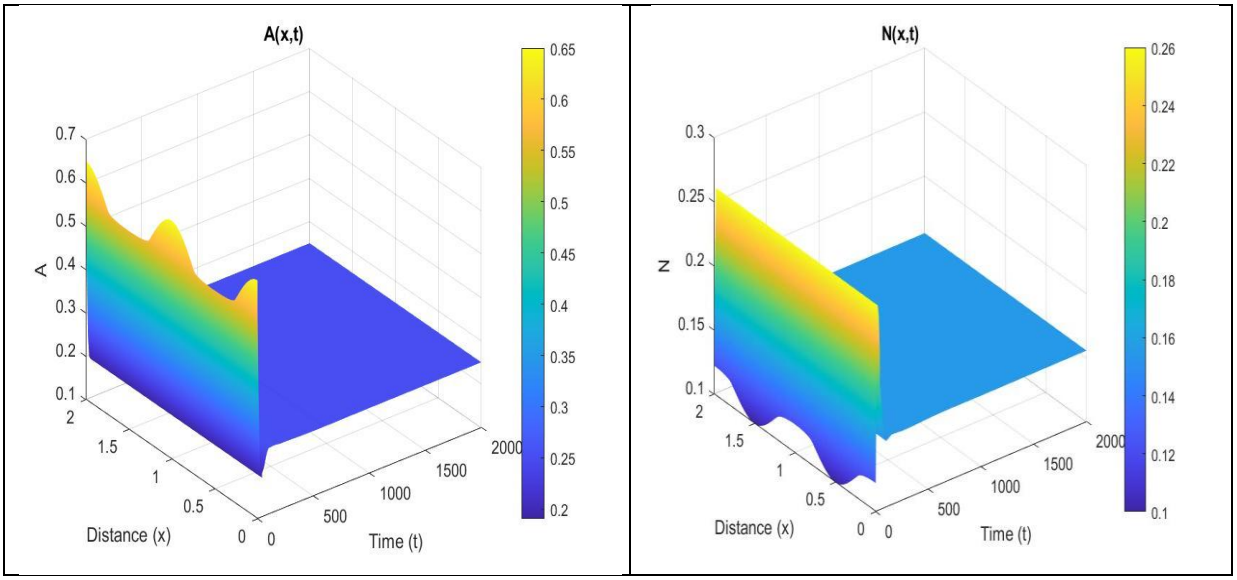

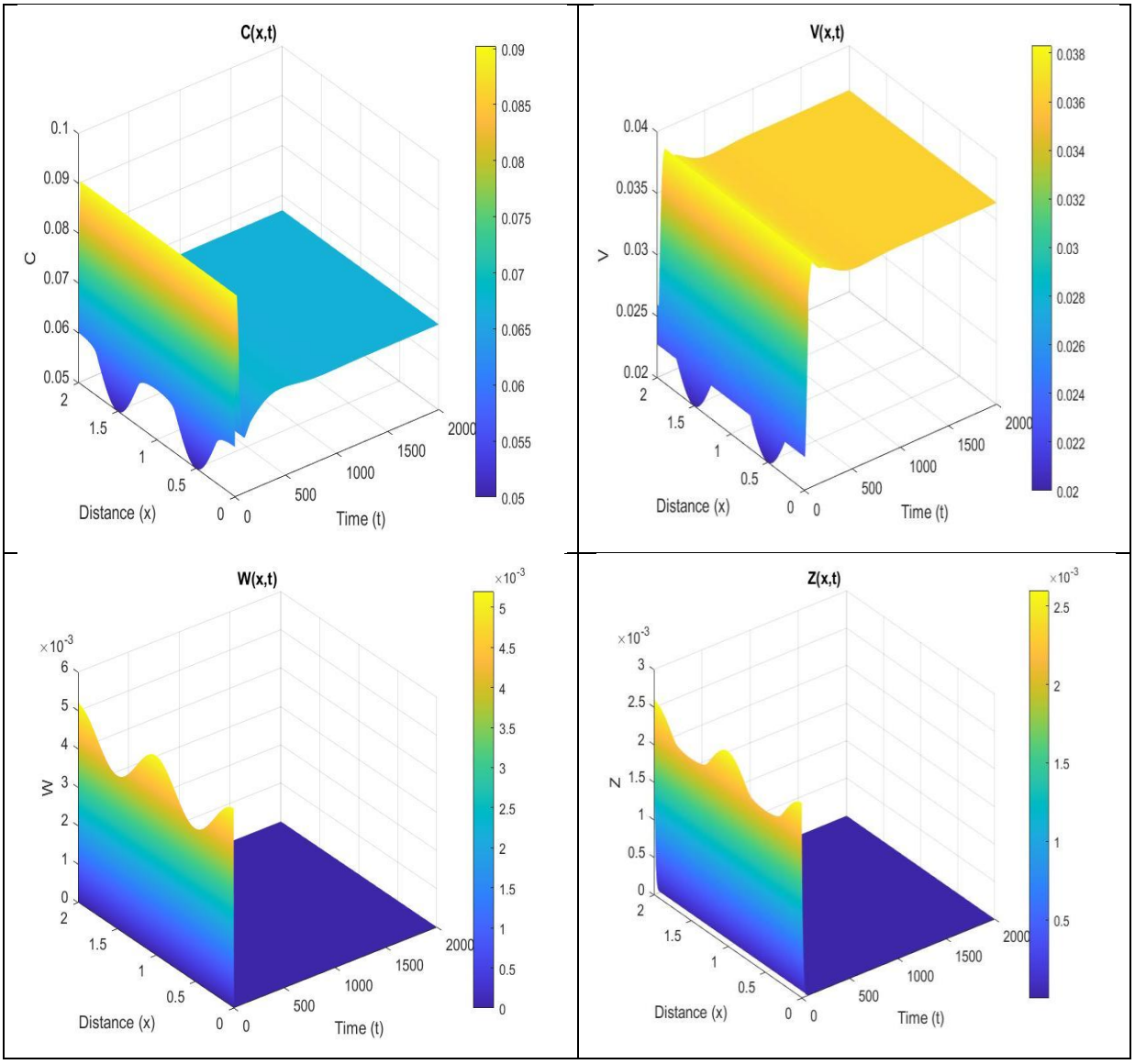

Figure 3: Numerical Simulations for Case-III by Hybrid Block method at k=0.001, n=101

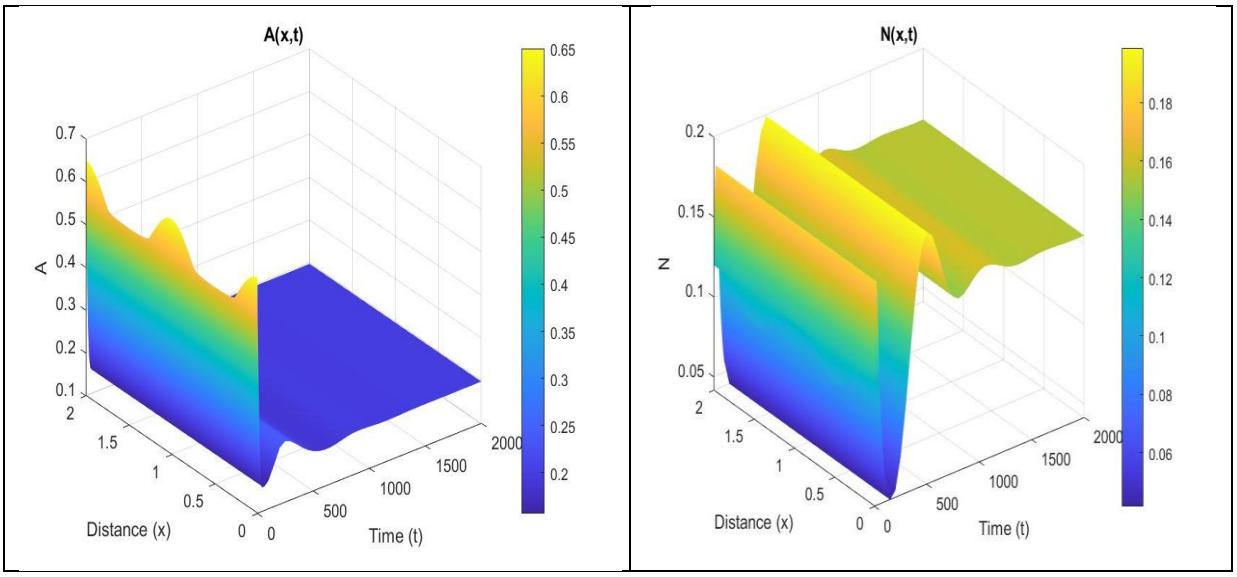

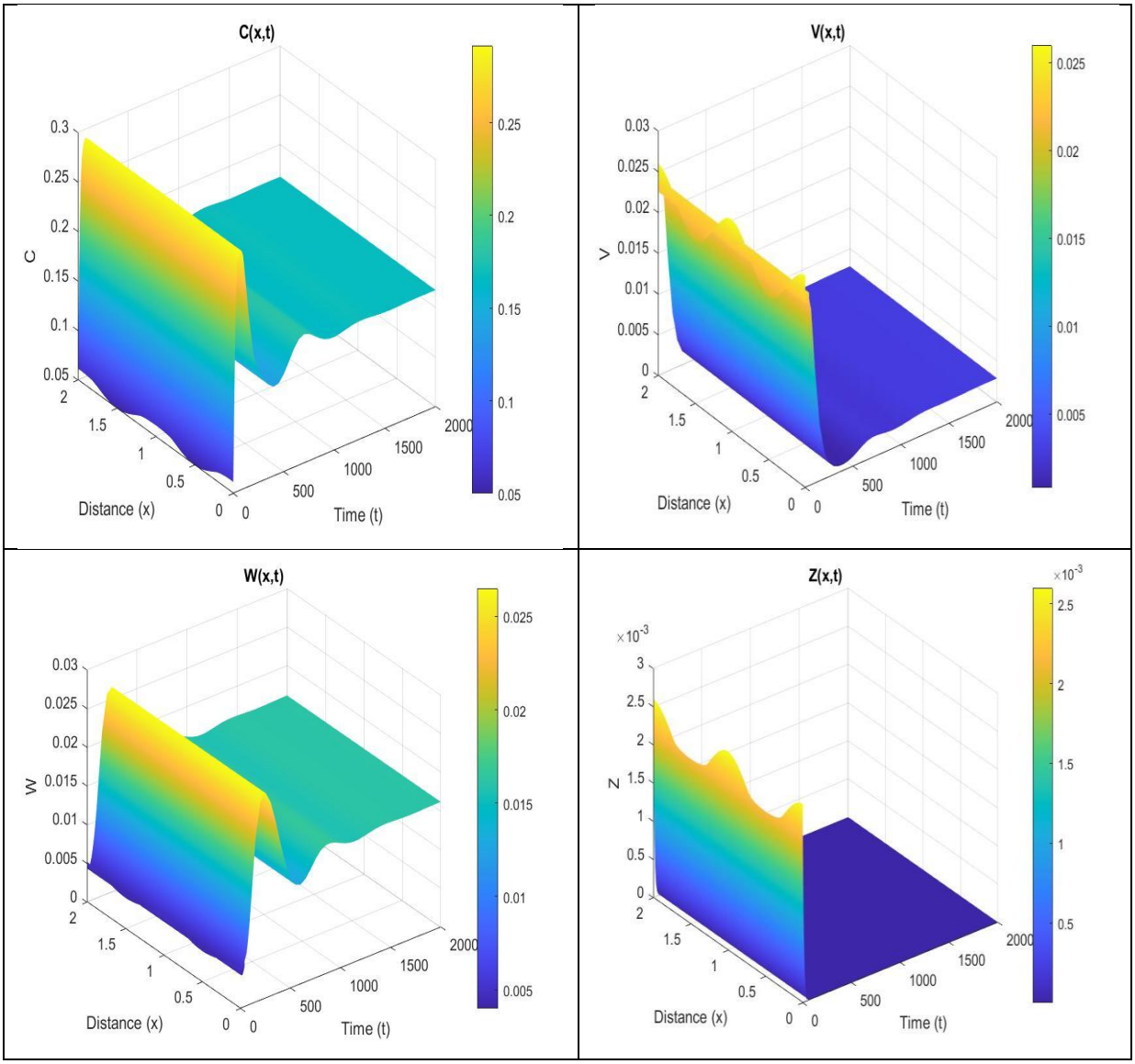

Figure 4: Numerical Simulations for Case-VI by Hybrid Block method at k=0.001, n=101

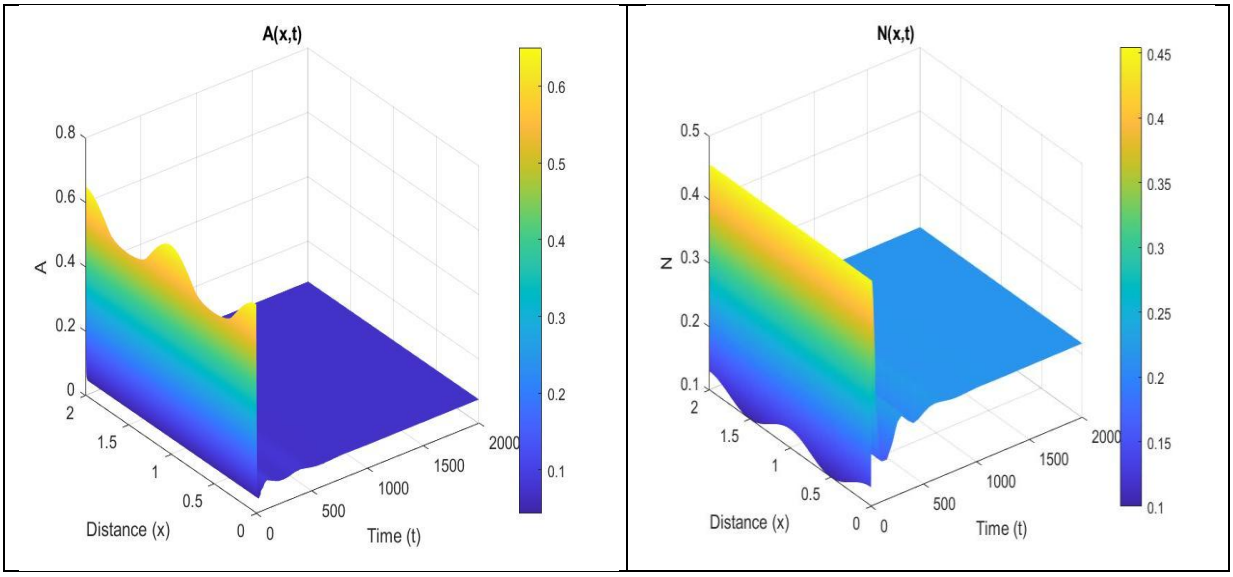

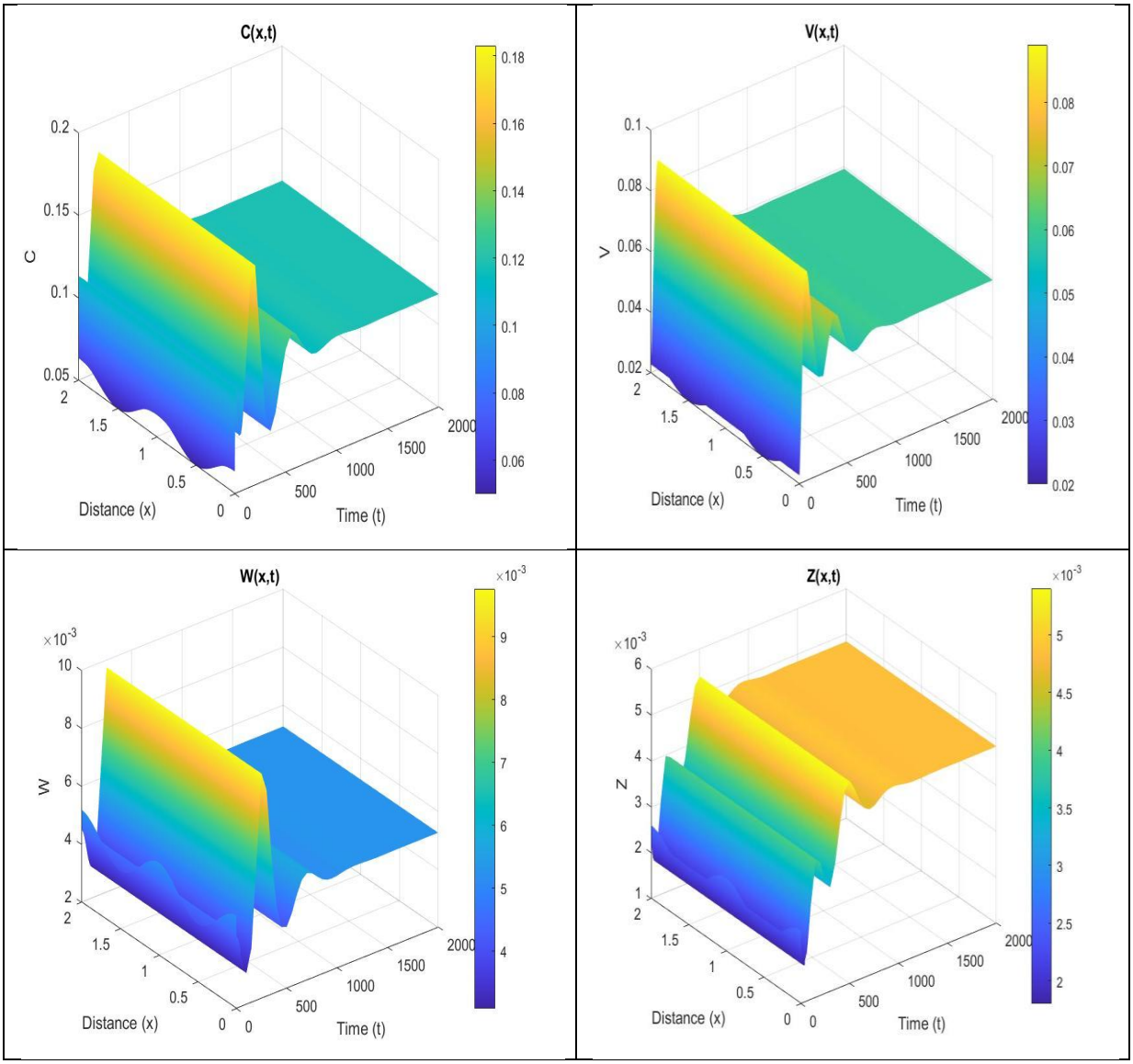

Figure 5: Numerical Simulations for Case-I by Hybrid Block method at k=0.001, n=51

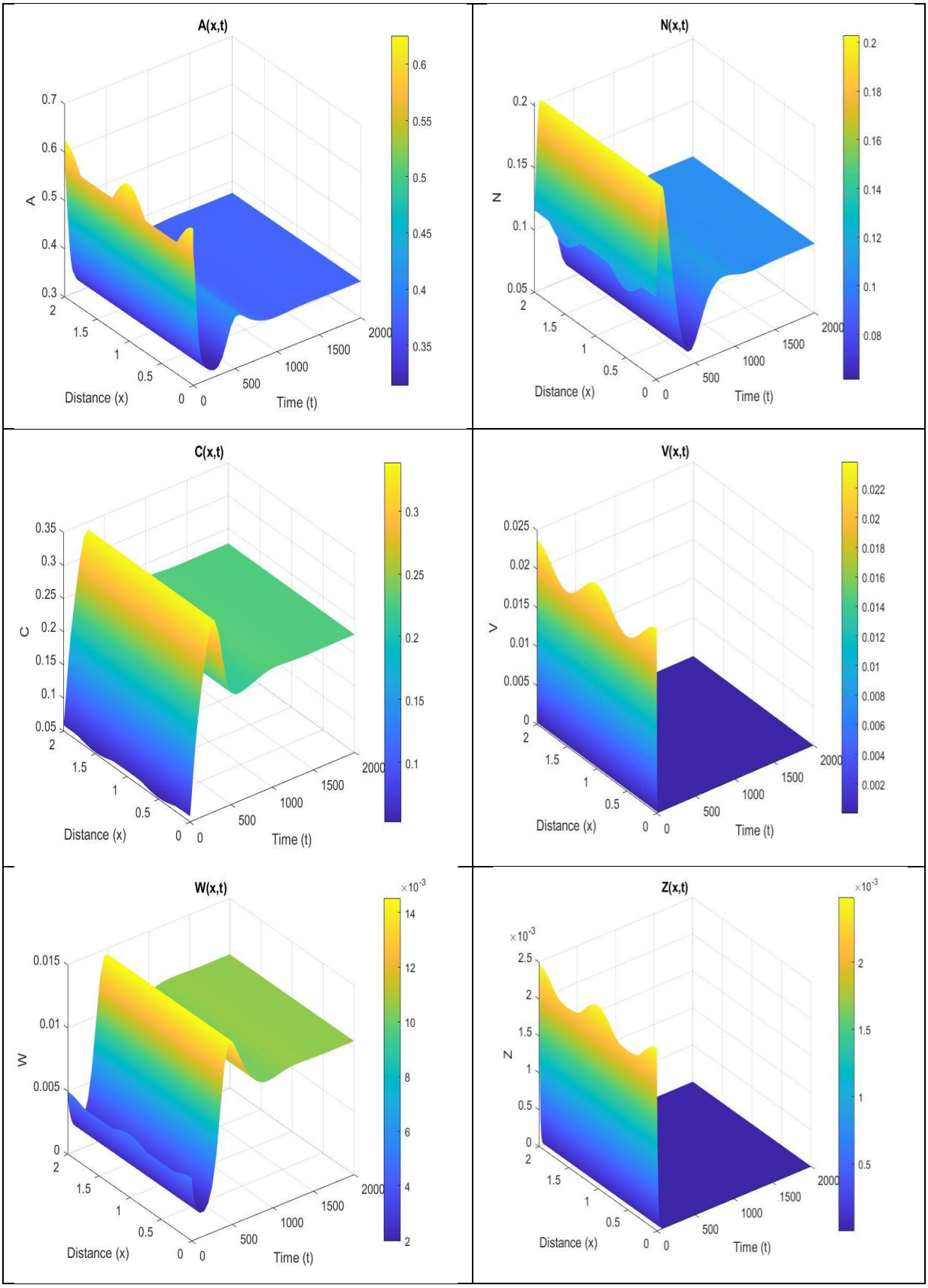
A(x,t)
A
Distance (x)
Time (t)
N(x,t)
N
Distance (x)
Time (t)
C(x,t)
C
Distance (x)
Time (t)
V(x,t)
V
Distance (x)
Time (t)
W(x,t)
W
Distance (x)
Time (t)
Z(x,t)
Z
Distance (x)
Time (t)

10. Conclusions

The given mathematical model describing the dynamics of the prevailing global pandemic coronavirus 2 (SARS-CoV-2) in cancer patients has been successfully numerically simulated by the proposed scheme of the collocation of the cubic B-splines followed by the hybrid block method. The key features of the proposed scheme are the well aptness of the cubic B-splines for such complex mathematical models. Moreover, the proposed technique is being implemented without using any of the linearising techniques to handle the non-linearity of the model. Achieving accurate solutions with higher order accuracy with less computational efforts and CPU time are the key benefits of the proposed methods. Such efficient approaches to simulate mathematical models describing the dynamics of like diseases can be of great importance for the biologists. The results of the proposed model can be well described biologically that can help the medical authorities to deal with such life-threatening diseases. Numerical simulation techniques to handle such mathematical models have always been a matter of concern and interest for the mathematician and the biological researchers of the field. Both the methods are therefore emerged as an alternative to deal with similar reaction-diffusion mathematical models [58, 59] emerging out from any practical real-world problem.

Availability of Data and Materials: All data generated or analysed in the present study are included and well referenced in this manuscript file.

Competing Interests: The authors declare that they have no competing interests.

Funding Statement: There is neither any fund grant nor any financial assistance received to conduct this research work.

Author's Contributions: RCM proposed the numerical scheme. RG and NA did all the computations and written the manuscript. The authors did the work on their mutual understanding without any conflicts.

Acknowledgements: The authors express their sincere gratitude towards their educational institutions for motivation and encouragement.

References

1. Hu B., Guo H., et al., Characteristics of SARS-Cov-2 and COVID-19, *Nature Reviews Microbiology,* 19, 141-154, 2021.
2. World Health Organization, Coronavirus. *World Health Organization cited January 19, 2020.* Available https://www.who.int/health-topics/coronavirus.
3. Hui D.S., et al., The continuing 2019-nCoV epidemic threat of novel coronaviruses to global health-the latest 2019 novel coronavirus outbreak in Wuhan, China, *Intl. J. Infect. Dis.,* 91, 264-266, 2020.
4. Gralinski L., Menachery V., Return of the Coronavirus: 2019-nCoV, *Viruses,* 12(2): 135, 2020.
5. National Health Commission of the People's Republic of China. Briefing on the latest situation of the novel coronavirus pneumonia epidemic. http://www.nhc.gov.cn/xcs/yqtb/list_gzbd.shtml 2020.
6. Nicola M., Alsafi Z., Sohrabi C. et al., The socio-economic implications of the coronavirus pandemic (COVID-19): A review, *International Journal of Surgery,* Vol. 78, 185-193, June 2020.
7. Alradhawi M., Shubber N., Sheppard J., Ali Y., Effects of the COVID-19 pandemic on mental well-being amongst individuals in society- A letter to the editor on "The socio-economic implications of the coronavirus and COVID-19 pandemic: A review", *International Journal of Surgery,* Vol. 78, 147-148, June 2020.
8. Pak A., Adegboye O.A., et al., Economic consequences to the COVID-19 outbreak: the need for epidemic preparedness, *Frontiers in Public Health* https://doi.org/10.3389/fpubh.2020.00241.
9. Syed Z., Syed Z., Impact of COVID-19 on IT, *Science Documents,* 1(3), December 2020.
10. Williams T., The impact of COVID-19, *Journal of Perioperative Practice,* 30(5), 114-115, May 2020.
11. Bhat R.A., Gulzar S., Muhee A., et al., Psychological Impacts of COVID-19, *Acta Scientific Veterinary Sciences,* Vol. 3, Issue 9, September 2021.

12. Ngima Y., Tsering D., Impact of COVID-19 on Education, *International Research Journal on Advanced Science Hub,* Vol. 2, ICAMET, 34-39, 2020.
13. Sackey P.A., Barfi R., The impact of Covid-19 pandemic on the global economy: Emphasis on poverty alleviation and economic growth, *Finance Research Letters,* 8(1). 32-43, January 2021.
14. Hui D.S., Azhar E.I., Madani T.A., Drosten C. et al., The continuing 2019-Ncov epidemic threat of novel coronavirus to global health the latest 2019 novel coronavirus outbreak in Wuhan China, *International Journal of Infectious Disease,* Vol. 91, No. 1, 264-266, 2020.
15. Huang C., Wang Y., Li X., Ren L., Zhao J., Hu Y., et al., Clinical features of patients infected with 2019 novel coronavirus in Wuhan, China, *The Lancet*, Vol. 395, Issue 10223, 497-506, 2020.
16. Chan J.F., Yuan S. et al., A familial cluster of pneumonia associated with the 2019 novel coronavirus indicating person-to-person transmission: a study of a family cluster, *The Lancet*, Vol. 395, Issue 10223, 514-523, 2020.
17. Sanyaolu A., et al., Comorbidity and its Impact on Patients with COVID-19, *SN Compr. Clin. Med.,* 2(8), 1069-1076, 2020.
18. Landman A., et al., Cancer patients in SARS-CoV-2 infection: A nationwide analysis in China, *Lancet Oncol.,* 21(30), 335-337, 2020.
19. Thibaudin M., et al., Immunological features of coronavirus disease 2019 in patients with cancer, *Eur. J. Cancer*, 139, 70-80, 2020.
20. Assaad S., et al., High mortality rate in cancer patients with symptoms of COVID-19 with or without detectable SARS-CoV-2 on RT-PCR, *Eur. J. Cancer*, 135, 251-259, 2020.
21. Indini A., et al., Coronavirus infection and immune system: An insight of COVID-19 in cancer patients, *Crit. Rev. Oncol. Hematol.,* 153, 103059, 2020.
22. Chen T.M., Rui J., Wang Q.P., Zhao Z.Y., Cui J.A. et al, A mathematical model for simulating the phase-based transmissibility of a novel coronavirus, *Infectious Diseases of Poverty*, Vol. 9, No. 1, 1-8, 2020.
23. Lin Q., Zhao S., Wang W. et al., A conceptual model for the coronavirus disease 2019 (COVID-19) outbreak in Wuhan, China with individual reaction and governmental action, *International Journal of Infectious Diseases,* Vol. 93, No. 1, 211-216, 2021.
24. Shatanawi W., Raza A., Arif M.S., et al., An effective numerical method for the solution of a stochastic coronavirus (2019-nCOVID) pandemic model, *Computers, Materials & Continua*, Vol. 66, No. 2, 1121-1137, 2021.
25. Raza A., Arif M.S., Rafiq M., A reliable numerical analysis for stochastic gonorrhea epidemic model with treatment effect, *International Journal of Biomathematics,* Vol. 2, No. 5, 445-465, 2019.
26. Ndairou F., Area I., Nieto J.A., Torres D.F.M., Mathematical modeling of COVID-19 transmission dynamics with a case study of Wuhan, *Chaos, Solitons & Fractals*, Vol. 135, 109846, June 2020.
27. Abdo M.S., Shah K., Wahash H.A., Panchal S.K., On a comprehensive model of novel coronavirus (COVID-19) under Mittag-Leffler derivative, *Chaos, Solitons & Fractals*, Vol. 135, 109867, June 2020.
28. Mohamadou Y., Halidou A., Kapen P.T., A review of mathematical modeling, artificial intelligence and datasets used in the study, prediction and management of COVID-19, *Applied Intelligence,* Vol. 50, 3913-3925, 2020.
29. Atangana A., Khan M.A., Modeling of the dynamics of novel coronavirus (2019-nCOV) with fractional derivative, *Alexandria Engineering Journal,* Vol. 59, No. 4, 2379-2389, 2020.
30. Shahid N., Baleanu D., Ahmed N. et al., Optimality of solution with numerical investigation for coronavirus epidemic model, *Computers, Materials & Continua,* Vol.67, No. 2, 2021.
31. Li C., et al., The within-host viral kinetics of SARS-CoV-2, *Math. Biosci. Eng.,* 17(4), 2853-2861.
32. Ke R., et al., Kinetics of SARS-CoV-2 infection in the human upper and lower respiratory tracts and their relationship with infectiousness, *MedRxiv.,* 1-26, https://doi.org/10.1101/2020.09.25.20201772, 2020.
33. Elaiw A.M., et al., Global stability of a within-host SARS-CoV-2/cancer model with immunity and diffusion, *Int. J. Biomathematics,* 2150093, DOI: 10.1142/S1793521500935,2021.
34. Kondo S., Miura T., Reaction-diffusion model as a framework for understanding biological pattern formation, *Science*, Vol. 329, Issue 5999, 1616-1620, 2010.
35. Hao W., Xue C., Spatial pattern formation in reaction-diffusion models: a computational approach, *Journal of Mathematical Biology*, 80(1-2), 521-543, 2020.

36. Cosner C., Reaction-diffusion-advection models for the effects and evolution of dispersal, *American Institute of Mathematical* Sciences, 34(5), 1701-1745, 2014.
37. Elaiw A.M., Agha A., Global analysis of a reaction-diffusion within host malaria infection model with adaptive immune responses, *MDPI Mathematics*, 8(563) 2020.
38. Elaiw A.M., hobiny A.D., Agha A., Global dynamics of reaction-diffusion oncolytic M1 virotherapy with immune responses, *Applied Mathematics and Computation*, 376, 124758, 2020.
39. Asif M., Jan S.U., Haider N., Al-Mdallal Q., Numerical modeling of NPZ-SIR models with and without diffusion, *Results in Physics*, 19, 103512, 2020.
40. Elaiw A.M., Alofi A.S., Global dynamics of secondary DENV infection with diffusion, *Hindawi: Journal of Mathematics*, Vol. 2021, 5585175, 2021.
41. Lanz A, Rogers D, Alford T L, An epidemic model of malware virus with quarantine 2019 *Journal of Advances in Mathematics and Computer Science*, Vol. 33, No. 4, pp. 1–10.
42. Xu Y H, Ren J G, Sun G Q, Propagation effect of a virus outbreak on a network with limited anti-virus ability 2016 *PLoS One*, Vol. 11, No. 10, pp. 1–18.
43. Liu J, Bianca C, Guerrini L, Dynamical analysis of a computer virus model with delays 2016 *Discrete Dynamics in Nature and Society*, Vol. 16, No. 1, pp. 1–19.
44. Pao C.V., Finite difference solutions of reaction-diffusion equations with continuous time delays, *Computers & Mathematics with Applications*, Vol. 42, Issue 3-5, 399-412, 2001.
45. Zhang R., Wang Z., Liu J., Liu L., A compact finite difference method for reaction-diffusion problems using compact integration factor methods in high spatial dimensions, *Advances in Difference Equations*, 274, 2018.
46. Yuan H, Chen G, Network virus-epidemic model with the point-to-group information propagation 2008 *Applied Mathematics and Computation*, Vol. 206, No. 1, pp. 357–367.
47. Unser M., Splines: a perfect fit for medical imaging, *Proceedings of SPIE, International Society of Optical Engineering*, 4684, 2002.
48. Mittal R.C., Jain R.K., Cubic B-splines collocation method for solving nonlinear parabolic partial differential equations with Neumann boundary conditions, *Communication in Nonlinear Science and Numerical Simulation*, 17(12), 4616-4625, December 2012.
49. Mittal R.C., Tripathi A., A collocation method for numerical solutions of coupled Burgers' equations, *International Journal for Computational Methods in Engineering Science and Mechanics*, 15, 457-71, 2014.
50. Mittal R.C., Jain R.K., Numerical solutions of nonlinear Burgers' equations with modified cubic B-spline collocation method, *Applied Mathematics and Computation*, 218(15), 7839-7855, April 2021.
51. Rohila R., Mittal R.C., Numerical study of reaction diffusion Fisher's equations by using B-spline method, *Crossmark: Mathematical Sciences*, 12, 79-89, 2018.
52. Mittal R.C., Jain R.K., Redefined cubic B-splines collocation method for solving convection-diffusion equations, *Applied Mathematical Modeling*, 36, 5555-73, 2012.
53. Mittal R.C., Arora G., Efficient numerical solution of Fisher's equations by using B-spline method, *International Journal of Computer Mathematics, Taylor & Francis*, 87, 3039-51, October 2010.
54. Hang H., Yao X., Li X., Articles M., Cubic B-spline curves and shape parameter and their applications, Hindawi: *Mathematical Problems in Engineering*, Vol. 2017, 3962617, 2017.
55. Ramos H., et al., Using a cubic B-spline method in conjunction with a one-step optimized hybrid block approach to solve nonlinear partial differential equations, *Comput. Appl. Math.*, 41:34, https://doi.org/10.1007/s40314-021-01729-7, 2022.
56. Martin A., Boyd I., Variant of the Thomas algorithm for opposite-bordered tri-diagonal system of equations, *International Journal for Numerical Methods in Biomedical Engineering* 26 (6), 752-9, 2010.
57. Cont S.D., Boor C., Elementary Numerical Analysis: An Algorithmic Approach, *McGraw-Hill Book Company*.
58. Mittal R.C., Goel R., Ahlawat N., An efficient numerical simulation of a reaction-diffusion malaria infection model using B-splines collocation, *Chaos, Solitons and Fractals*, 143 (110566), 2021.
59. Goel R., Mittal R.C., Ahlawat N., Numerical simulation of oncolytic M1 cancer virotherapy reaction-diffusion model by collocation of B-splines, *Turkish Journal of Computer and Mathematics Education*, 13 (02), 451-474, 2022.